for data from the literature. These figures bear out the fact that for the compounds and temperature ranges examined, the data obtained in this study are as good or better than those available elsewhere in the literature.

The raw vapor pressure data for the three binary systems are presented in Table III. To simplify the notation, isobutane, 1-butene, and 1,3-butadiene are referred to as components 1, 2, and 3, respectively.

Binary data for these systems are extremely limited. Karabanov and Zorin (*5*) measured vapor–liquid equilibrium data for these systems; however, since their temperatures were all below 0 °C their results cannot be directly compared to the data of this study.

Laurance and Swift (*6*) have thoroughly studied the binary 1,3-butadiene–1-butene system. The results of their study, as shown in Figure 7, are somewhat different from the results of this study, and their pure component vapor pressure data for 1,3-butadiene are high in comparison with most literature sources at 100 °F.

The raw vapor pressures for the four ternary mixtures studied are presented in Table IV.

Conclusions

An apparatus capable of determining vapor pressures with a probable error of ±0.05% over a range of 40–160 °F and 20–160 psia is demonstrated by a significant amount of new vapor pressure data for the 1-butene, isobutane, 1,3-butadiene system. The laboratory technique should be of interest to other experimenters, and the new data should help improve correlations of vapor pressures for the systems studied. The data are also of use in calculating equilibrium vapor compositions to be used in the design of separation equipment.

Literature Cited

(1) Beattie, J. A., Marple, Jr., S., *J. Am. Chem. Soc.*, **72,** 1449 (1950).
(2) Beattie, A., Edwards, D. G., Marple, Jr., S., *J. Chem. Phys.*, **17,** 576 (1949).
(3) Dana, L. I., Jenkins, A. C., Burdick, J. N., Timm, R. C., *Refrig. Eng.*, **12,** 387 (1926).
(4) Goff, G. H., Farrington, P. S., Sage, B. H., *Ind. Eng. Chem.*, **42,** 735 (1950).
(5) Karabanov, N. T., Zorin, A. D., *Tr. polhim. Khim Tech.*, **1,** 3 (1964).
(6) Laurance, D. R., Swift, G. W., *J. Chem. Eng. Data*, **19,** 61 (1974).
(7) Manley, D. B., M.S. Thesis, The University of Kansas, 1968.
(8) Meyers, C. H., Jessup, R. S., *J. Res. Natl. Bur. Stand.*, RP324, **6,** 1061 (1935).
(9) Morris, W. M., Sage, B. H., Lacey, W. N., *Trans. Am. Inst. Min. Metall. Eng.*, **136,** 158 (1940).
(10) Olds, R. H., Sage, B. H., Lacey, W. H., *Ind. Eng. Chem.*, **38,** 301 (1946).
(11) Sage, B. H., Lacey, W. N., *Ind. Eng. Chem.*, **30,** 673 (1938).
(12) Scott, R. B., Meyers, C. H., Rands, Jr., R. D., Brickwedde, F. G., Bekkedahl, N., *J. Res. Natl. Bur. Stand.*, RP1661, 35 (1939).
(13) Siebert, F. M., Burrell, G. A., *J. Am. Chem. Soc.*, **37,** 2683 (1915).
(14) Walker, S. L., M.S. Thesis, The University of Missouri-Rolla, 1973.

Received for review July 14, 1975. Accepted June 21, 1976.

Acknowledgment is made to the University of Missouri-Rolla, Department of Chemical Engineering for financing the computational services and to the donors of the Petroleum Research Fund, administered by the American Chemical Society, for partial support of this research.

Viscosity of Methane, Hydrogen, and Four Mixtures of Methane and Hydrogen from −100 °C to 0 °C at High Pressures

Sheng-yi Chuang,[†] Patsy S. Chappelear,[‡]* and Riki Kobayashi*

William Marsh Rice University, Chemical Engineering Department, Houston, Texas 77001

The absolute capillary method was used to measure the viscosity of methane, hydrogen, and mixtures nominally 20, 40, 60, and 80% hydrogen at 0, −50, −75, and −100 °C at pressures from 4 atm up to 450–500 atm. The maximum probable error of the calculated viscosity is estimated to be 0.5%. The viscosity data were fit by the least-squares method to give 1.193 ± 0.034 for the Hagenbach factor for the kinetic correction in the vicosity formula. The residual viscosity concept was obeyed within ±1% except for hydrogen and the 80% hydrogen mixture. The deviations for these are attributed to first-order quantum effects.

The earliest investigations (*21, 36, 37, 41, 43–45*) of viscosity were at atmospheric pressure; Michels and co-workers (*30, 32*) were among the first to extend investigations to high pressures. The first low temperature–high pressure investigation reported was by Ross and Brown (*38*) in 1957; however, their data are now regarded (*9, 14, 25*) to be in serious error. A modification of the Rankine type viscometer using positive displacement pumps was used in separate investigations by Flynn et al. (*9*) at −78.5 to 100 °C below 200 atm and by Kao and Kobayashi (*25*) to reach −90 °C below 200 atm.

The falling body viscometer, which is not an absolute instrument, was used by Huang, Swift, and Kurata (*17*) from −170 to 0 °C up to 5000 psi. Kestin and co-workers (*22, 26*) have developed the oscillating-disk viscometer for absolute measurements at room temperature and higher. The concentric cylinder viscometer first used by Couette (*7*) has not been adapted to low temperature–high pressure investigations. Barr (*1*) gives detailed accounts of the various methods for measuring viscosity.

Experimental Details

A schematic of the equipment is shown in Figure 1. Earlier investigations at essentially room temperature on a similar installation were reported by Giddings (*10, 11*) for methane and propane. Placement of the pumps into the same temperature bath as the capillary by Kao et al. (*25*) led to investigations (*23, 24*) on helium, nitrogen, and their mixtures. Significant expermental difficulties arose as the temperature of investigation decreased.

The equipment consists of (1) a stainless steel capillary cell in which a Pyrex glass capillary is held, (2) a pair of coupled flow generating pumps maintained in the same temperature bath as the capillary cell, (3) a dead weight gage system for pressure measurement, (4) a differential pressure measuring system, (5)

[†] Present address: 8819 Haverstock, Houston, Texas 77071.
[‡] Address correspondence to this author at McDermott Hudson Engineering Corp., Houston, Texas 77036.

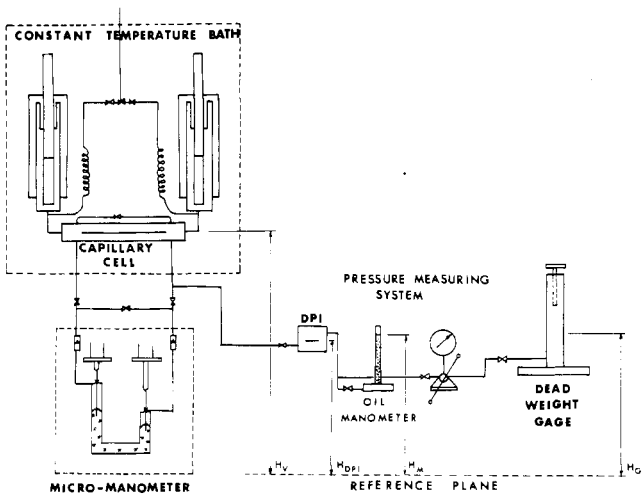

Figure 1. Schematic of experimental capillary viscometric system: DPI = differential pressure indicator; H_V, H_{DPI}, H_M, H_G = heights needed in calculation of pressure measured by dead weight gage.

a temperature control and measuring system, and (6) a gas charging system. During this investigation a high accuracy micromanometer (*40*) was designed and constructed. The manometer is enclosed in an air bath regulated to ±0.1 °C; it has an accuracy of ±2 μ in a total differential pressure range of 96 mmHg. For extensive details on other equipment problems, the reader is referred to the theses (*5, 10, 23*), which are available from University Microfilms. In particular, ref 5 reports cryogenic valves, packing design for the pumps, and leaks from chrome-plated plungers in the pumps. The plated plungers were replaced with homogeneous plungers made of 440A stainless steel, heat treated to 54C Rockwell hardness.

This type of leakage through the "porous" chrome plating was observed during the development of another apparatus in this laboratory, the micropump (*39*). The leak can be measured with the micropump, which can produce flow rates from 0.36 to 8 × 10^{-8} cm^3 min^{-1}.

The viscosity measurements at 0 and −50 °C up to 500 atm, as indicated in the data tables, were made before this replacement with appropriate correction for the leak rate being made by the leak rate studies. Measurements made after the replacement with homogeneous plungers required no leak correction.

Calculation of Viscosity. The theory of capillary viscometry was treated in an extensive review by Kestin et al. (*27*) after the completion of the study reported here. The data of this paper were calculated from the Hagen-Poiseuille law (*1, 15, 34*) with several correction factors as

$$\mu = \frac{\pi \bar{a}^4 \Delta P(1 + 4\zeta/\bar{a}) C_{PY}^3}{8(L + n\bar{a}) Q_P \zeta} - m \frac{\rho Q_P \ln (P_1/P_2)}{8\pi(L + n\bar{a}) C_{PY}} \quad (1)$$

or

$$\mu = \mu_P - m\mu_K \quad (2)$$

The working equation of Kestin et al. (*27*) is given by

$$\mu = \frac{\pi a^4 \rho}{8(L + na)} \left[\frac{\Delta P}{\dot{m}} - \frac{m_0 \dot{m}}{\rho \pi^2 a^4} \right] \quad (3)$$

where $\dot{m}$ is the measured mass flow rate and m_0 is defined by *m, n,* and the Reynolds number. Equations 1 and 3 can be shown to be equivalent.

The correction term *m* is usually referred to as the Hagenbach (*15*) factor for the loss in kinetic energy. Earlier work on this subject was reported by Barr (*1*). Erk (*8*) showed that *m* should not be equal to 1.

The nonuniformity of the capillary bore is the term ξ = 1.000 352 with $\bar{a}$ as the mean radius of the capillary determined by the electrical resistance method using mercury as the conducting fluid.

When the pressure drop ΔP is large relative to the system pressure and/or the compressibility changes by an appreciable amount down the capillary, corrections for averaging the compressibility must be made. Erk (*8*) also included the correction for compressible gases in his treatment of the kinetic correction to viscometric equations. A small logarithmic term ln P_1/P_2 is added to the Hagenbach factor, where 1 and 2 denote the ends of capillary. In this work these corrections were negligible.

A fictitious length $n\bar{a}$, the Couette (*7*) correction, must be added to the length *L* of the capillary to account for the viscous dissipation of energy at the inlet of the capillary. Weissberg (*47*) showed in a theoretical study that *n* ranges from 1.17 for L/a = 0 to 1.36 as $L/a \rightarrow \infty$ for a square ended tube. In this work 1.2 was used for *n*, which amounts to a 0.025% correction in the viscosity. Kestin et al. (*27*) report the theoretical value of *n* as 0.69.

Knudsen (*28*) showed that a correction $4\zeta/\bar{a}$ is required for slippage at the wall of the capillary. The maximum slip correction in this work is 0.21% for hydrogen at 0 °C and 4 atm. Thornton and Dunlop (*42*) report some interesting results for the slip correction for some studies at atmospheric pressure.

The Pyrex materials of the capillary and the steel of the pump plungers change dimension with pressure and temperature. The corrections C_{PY} and C_{ST} were obtained from literature values (*3, 4, 20*).

The pressure drop ΔP was obtained from the micromanometer (*40*) difference Δh

$$\Delta P = \Delta h(\rho_{Hg} - \rho_m)g$$

where the density of mercury ρ_{Hg} and of the gas ρ_m are taken at the pressure *P* and the manometer temperature of 40 °C. Other terms in the equation are the density ρ of the gas at system conditions and the volumetric flow rate Q_P.

Correction for Leaks with Plated Plungers. All of the previous corrections discussed would have to be considered for any experimental apparatus. This experiment required one additional correction: that for the leak from the pumps during the initial 0 and −50 °C investigations. The correction *q* in terms of the difference in the equilibrium pressure of the system before and after the viscosity measurement is given by

$$q = 0.22 \frac{V_T}{P} \frac{\Delta P}{\Delta t}$$

where V_T is the total volume of the fluid in the system, that at the bath temperature, that in the connecting tubing, and that at the manometer temperature. ΔP is the change in the pressure *P* for the time Δt. The constant 0.22 arises from consideration of the relative leak rates from the plunger on each side of the tandem pump. The leak rate varied from 0.1 to 1.5 cm^3 h^{-1} at 0 °C.

The correction term *q* is added to Q_P in eq 1 for the measurements made with the plated plungers. The agreement between viscosity data obtained with a leak and without a leak existing at the same conditions shows that the correction is applicable. The pressure at which the measurement is made is also derived in terms of the leak rate and initial conditions.

Gases Studied. "Ultrahigh purity grade" methane (99.97 mole % pure) and hydrogen (99.999 mole % pure) were supplied by the Matheson Gas Company. Mixtures were prepared by Matheson to be as close as possible to the original composition of the experimental compressibility data of Mueller (*33*). The supplier made an analysis by gas chromatography, Monsanto Chemical Company provided two mass spectrometric analyses, and an analysis was made in this laboratory by Teh-Cheng Chu using gas chromatography. The compositions of mixtures A, B, C, and D used for the calculations were 19.42, 33.75, 53.37, and 78.70 mole % hydrogen.

Table I. Viscosity of Methane–Hydrogen System, Composition = 0.00 Mole % Hydrogen

Temp = 273.15 K			Temp = 223.15 K			Temp = 198.15 K			Temp = 173.15 K		
Pressure, atm	Density, g cm^{-3} ×10^3	Viscosity,[a] μP	Pressure, atm	Density, g cm^{-3} × 10^3	Viscosity,[a] μP	Pressure, atm	Density, g cm^{-3} × 10^3	Viscosity,[a] μP	Pressure, atm	Density, g cm^{-3} × 10^3	Viscosity,[a] μP
4.014	2.90	102.07	4.009	3.58	85.02	4.014	4.07	76.39	4.007	4.71	66.72
10.003	7.34	102.95	10.004	9.19	85.85	9.998	10.58	77.54	9.995	12.61	67.66
19.989	15.03	104.54	40.016	44.00	95.14	20.012	23.05	80.22	19.984	29.78	70.59
39.960	31.63	109.63	79.926	126.16	137.65	39.993	59.78	92.19			
59.819	49.83	115.97	99.904	177.87	181.75	59.957	197.91	195.06			
99.879	91.36	133.08	139.877	235.40	248.48	70.025	235.89	243.62			
139.866	134.91	163.81	199.703	274.37	312.03	99.792	273.69	306.79			
199.780	188.38	210.40	299.449	308.70	385.68	138.977	297.18	357.42			
299.247	242.24	276.63	399.551	330.44	445.83	199.627	319.23	411.15			
399.496	275.04	330.86	499.182	346.47	498.75	299.422	342.41	485.05			
499.132	297.90	376.80				399.280	358.68	547.73			
						495.404	371.30	607.55			

[a] Accuracy of viscosity ≈0.5%. One additional figure is given to avoid round off error.

Table II. Viscosity of Methane–Hydrogen System, Composition = 19.42 Mole % Hydrogen

Temp = 273.15 K			Temp = 223.15 K			Temp = 198.15 K			Temp = 173.15 K		
Pressure, atm	Density, g cm^{-3} × 10^3	Viscosity,[a] μP	Pressure, atm	Density, g cm^{-3} × 10^3	Viscosity,[a] μP	Pressure, atm	Density, g cm^{-3} × 10^3	Viscosity,[a] μP	Pressure, atm	Density, g cm^{-3} × 10^3	Viscosity,[a] μP
4.014	2.40	103.99	4.023	2.96	86.96	4.001	3.34	77.81	4.007	3.86	68.19
10.015	6.04	104.45	10.014	7.52	87.58	10.008	8.58	78.57	10.002	10.05	69.08
19.996	12.24	105.84	19.984	15.51	89.11	19.983	17.99	80.41	34.947	42.33	77.65
39.970	25.18	109.20	39.917	33.20	94.00	39.964	40.18	86.55			
59.952	38.77	113.53	59.889	53.49	101.22	59.954	69.18	98.11			
99.831	67.32	125.06	99.843	100.96	124.46	99.945	141.22	145.97			
199.764	135.81	165.93	199.960	195.41	204.15	199.894	233.92	252.95			
299.536	184.80	208.95	299.747	240.85	264.50	299.433	270.44	318.00			
399.376	218.09	247.33	398.605	266.49	313.90	399.229	293.56	371.22			
498.577	242.35	284.19	499.022	286.95	354.51						

[a] Accuracy of viscosity ≈0.5%. One additional figure is given to avoid round off error.

Densities and compressibilities required for the calculations were obtained from Michels et al. (*31*) for hydrogen, from Vennix et al. (*46*) for methane, and from the Pope et al. (*35*) analysis of the Mueller (*33*) data for the mixtures.

Sequence of Experiments. At each temperature investigated the gases were studied in the order of increasing hydrogen content. The first measurements were made at 0 and −50 °C from 4 to 500 atm. Since these measurements were made before the leakage problem was solved, a correction factor was added in the viscometric equation. After the fabrication and installation of the homogeneous plungers, the correction was no longer necessary. Measurements from 4 to 500 atm were made at −75 and at −100 °C up to the gas–liquid equilibrium region for methane and the two-phase region for mixtures A and B, and up to 450 atm for mixtures C and D and hydrogen. After the low temperature measurements, measurements for methane at 0 and −50 °C and for hydrogen at −50 °C were made to check the values obtained at the beginning of the experimental work. The average agreement between the two sets of data was ±0.1%. In addition, repeated measurements either with the same or a different flow rate were frequently made to check the experimental consistency. The average reproducibility was ±0.05%.

Results

The calculated values for the viscosity of the gases at two various experimental conditions are given in Tables I to VI. Basic data are available in the thesis (*5*). A detailed error analysis considered the various variables involved in the measurements; e.g., capillary length, uniformity, constant flow rate, etc., and showed that the most significant error arose from the determination of the positions of the mercury meniscus in the manometer. The result of this error analysis was a maximum relative error of the viscosity or ±0.103% with an average reproducibility of ±0.05%, which may be taken as a measure of the precision. However, a later analysis of these data (*16*) which considered critical effects has shown that the actual error is more of the order of ±0.5%.

However, one should note that the results of this study are not sufficiently close to the critical region where numerical integration is required. Values of $\Delta P_P/\Delta P$ reported in Table VIII show that numerical integration is not justified for these data.

Hagenbach Factor. The data from the measurements with the homogeneous plungers were used to evaluate the Hagenbach factor. Transposing terms in eq 2 gives

$$\mu_P = \mu + m\mu_K \tag{4}$$

From two measurements 1, 2 at the same T, P conditions but with different flow rates, m can be obtained as the simple slope from the linear equation. Initially ten sets of data which contained either x or y of a magnitude less than the calculated experimental accuracy of the viscosity were discarded. The least-squares method was used to compute m. After the first trial fit, 12 points which were outside the range of five times the standard deviation were discarded. The remaining 30 points were used to obtain $m = 1.193 \pm 0.034$, as shown in Figure 2. Kestin et al. (*27*) report $m = 1.17$ as the theoretical value.

Pressure Relationship. Figures 3 and 4 for methane, Figure

Table III. Viscosity of Methane–Hydrogen System, Composition = 33.75 Mole % Hydrogen

Temp = 273.15 K			Temp = 223.15 K			Temp = 198.15 K			Temp = 173.15 K		
Pressure, atm	Density, g cm^{-3} × 10^3	Viscosity,[a] μP	Pressure, atm	Density, g cm^{-3} × 10^3	Viscosity,[a] μP	Pressure, atm	Density, g cm^{-3} × 10^3	Viscosity,[a] μP	Pressure, atm	Density, g cm^{-3} × 10^3	Viscosity,[a] μP
4.012	2.03	104.11	4.019	2.50	87.46	4.008	2.82	78.86	4.008	3.25	69.33
9.994	5.09	104.69	10.006	6.30	87.92	10.014	7.19	79.47	9.995	8.34	70.01
19.994	10.25	105.78	19.994	12.83	89.29	19.987	14.81	80.92	19.983	17.57	71.66
39.962	20.79	108.42	39.970	26.64	93.08	39.967	31.63	85.11	29.958	27.92	74.06
99.877	53.43	119.85	59.911	41.38	98.02	59.891	50.60	91.73	39.941	39.69	77.43
199.778	105.24	147.08	99.920	73.03	111.48	99.862	93.67	112.86	44.937	45.94	79.58
299.603	146.35	177.39	199.637	143.47	159.11	199.741	176.22	180.55	49.929	53.28	82.28
399.356	177.08	206.27	300.101	188.82	203.87	299.586	217.81	234.94			
498.704	200.58	233.20	399.023	214.97	240.82	399.564	244.01	277.77			
			498.946	241.69	274.63						

[a] Accuracy of viscosity ≈0.5%. One additional figure is given to avoid round off error.

Table IV. Viscosity of Methane–Hydrogen System, Composition = 53.37 Mole % Hydrogen

Temp = 273.15 K			Temp = 223.15 K			Temp = 198.15 K			Temp = 173.15 K		
Pressure, atm	Density, g cm^{-3} × 10^3	Viscosity,[a] μP	Pressure, atm	Density, g cm^{-3} × 10^3	Viscosity,[a] μP	Pressure, atm	Density, g cm^{-3} × 10^3	Viscosity,[a] μP	Pressure, atm	Density, g cm^{-3} × 10^3	Viscosity,[a] μP
4.001	1.53	103.85	4.013	1.88	87.70	4.002	2.12	78.96	4.002	2.43	70.29
10.008	3.83	104.13	10.005	4.72	88.05	9.986	5.34	79.45	9.990	6.15	70.81
19.986	7.65	104.72	19.965	9.48	88.83	19.980	10.83	80.41	19.986	12.56	71.95
39.934	15.31	106.56	39.967	19.26	90.54	39.969	22.27	83.15	39.982	26.24	75.44
99.893	38.11	113.14	59.888	29.19	92.91	59.934	34.19	86.80	59.936	40.46	80.21
199.650	73.25	129.05	99.952	49.32	101.08	99.846	58.68	96.24	99.849	71.50	94.38
299.301	102.79	146.62	199.767	95.13	124.17	199.795	112.41	127.87	139.788	100.47	112.50
399.298	126.99	164.59	299.655	130.10	151.26	299.684	149.51	159.64	199.751	135.93	139.47
499.225	146.82	181.79	399.422	156.09	174.56	399.503	175.45	188.87	299.541	177.21	178.49
			498.978	176.21	196.30	499.245	196.14	213.92	399.472	204.08	211.56
									449.314	213.74	226.79

[a] Accuracy of viscosity ≈0.5%. One additional figure is given to avoid round off error.

Table V. Viscosity of Methane–Hydrogen System, Composition = 78.70 Mole % Hydrogen

Temp = 273.15 K			Temp = 223.15 K			Temp = 198.15 K			Temp = 173.15 K		
Pressure, atm	Density, g cm^{-3} × 10^3	Viscosity,[a] μP	Pressure, atm	Density, g cm^{-3} × 10^3	Viscosity,[a] μP	Pressure, atm	Density, g cm^{-3} × 10^3	Viscosity,[a] μP	Pressure, atm	Density, g cm^{-3} × 10^3	Viscosity,[a] μP
4.019	0.90	99.05	3.992	1.09	85.30	4.009	1.23	77.24	4.009	1.41	69.35
10.000	2.22	99.15	9.994	2.73	85.45	10.003	3.07	77.67	10.000	3.52	69.55
19.991	4.42	99.38	19.989	5.44	85.62	19.978	6.13	78.25	19.988	7.04	70.26
39.950	8.76	100.23	39.901	10.79	86.68	39.972	12.21	79.46	39.951	14.06	71.79
99.843	21.25	103.34	99.900	26.36	90.96	59.904	18.17	81.01	59.923	21.00	73.82
199.751	40.19	110.21	199.736	49.56	100.60	99.864	29.83	84.68	99.836	34.45	78.77
299.501	56.64	118.15	299.540	68.90	110.87	199.717	55.80	96.71	139.809	47.04	84.58
399.271	70.66	126.49	399.133	84.82	122.32	299.610	76.72	109.78	199.690	63.79	93.93
499.025	82.48	134.88	499.072	98.18	132.82	399.369	93.42	122.80	299.543	85.92	110.10
						499.249	107.15	134.56	399.450	103.23	125.86
									449.273	110.35	133.30

[a] Accuracy of viscosity ≈0.5%. One additional figure is given to avoid round off error.

5 for hydrogen, and Figure 6 for the mixtures at −75 °C show the results along with comparison with other data. The viscosity of methane depends much more strongly on pressure than the viscosity of hydrogen. There is an apparent initial decrease in the viscosity with increase in pressure for hydrogen at 0 and −50 °C but not at −75 or −100 °C. However, the magnitude of the decrease is only 0.05% of the value of the viscosity, which is less than the experimental accuracy; however, similar observations were seen by others. They were reported by Barua et al. (*2*) at 150 °C for hydrogen, by Kao and Kobayashi (*24*) at 50 °C for helium, by Kestin and Leidenfrost (*26*) at 20 °C for helium, and by Flynn et al. (*9*) and Gracki et al. (*14*) at −25 and 100 °C for helium.

Composition Relationship. Examples of the isobaric isothermal behavior are shown in Figures 7 and 8. A maximum occurs in the viscosity at low pressures.

Temperature Relationship. For purposes of illustration isobaric plots of the viscosity of methane vs. temperature are shown in Figure 9.

Density and Residual Viscosity Relationship. The zero

Table VI. Viscosity of Methane–Hydrogen System, Composition = 100.00 Mole % Hydrogen

Temp = 273.15 K			Temp = 223.15 K			Temp = 198.15 K			Temp = 173.15 K		
Pressure, atm	Density, g cm^{-3} × 10^3	Viscosity,[a] μP	Pressure, atm	Density, g cm^{-3} × 10^3	Viscosity,[a] μP	Pressure, atm	Density, g cm^{-3} × 10^3	Viscosity,[a] μP	Pressure, atm	Density, g cm^{-3} × 10^3	Viscosity,[a] μP
4.021	0.36	83.23	4.004	0.44	72.95	3.991	0.49	67.03	4.005	0.57	60.71
10.002	0.89	83.20	9.993	1.09	72.82	9.990	1.23	67.11	9.993	1.41	60.91
19.982	1.78	83.27	19.981	2.17	72.95	19.973	2.44	67.28	19.944	2.79	61.22
39.962	3.51	83.48	39.927	4.28	73.29	39.965	4.82	67.82	39.945	5.51	61.77
79.841	6.83	84.08	99.772	10.24	74.87	99.818	11.50	69.78	59.901	8.14	62.56
119.629	9.98	85.17	199.688	19.06	78.56	199.763	21.25	74.37	99.872	13.14	64.38
199.677	15.84	87.42	299.556	26.59	83.14	299.497	29.39	79.64	139.807	17.76	66.40
399.273	28.11	94.63	399.342	33.06	88.16	399.303	36.27	85.55	199.702	24.04	69.98
498.152	33.18	98.25	499.260	38.69	93.18	499.218	42.16	91.26	299.550	32.92	76.53
									399.422	40.22	83.53

[a] Accuracy of viscosity ≈0.5%. One additional figure is given to avoid round off error.

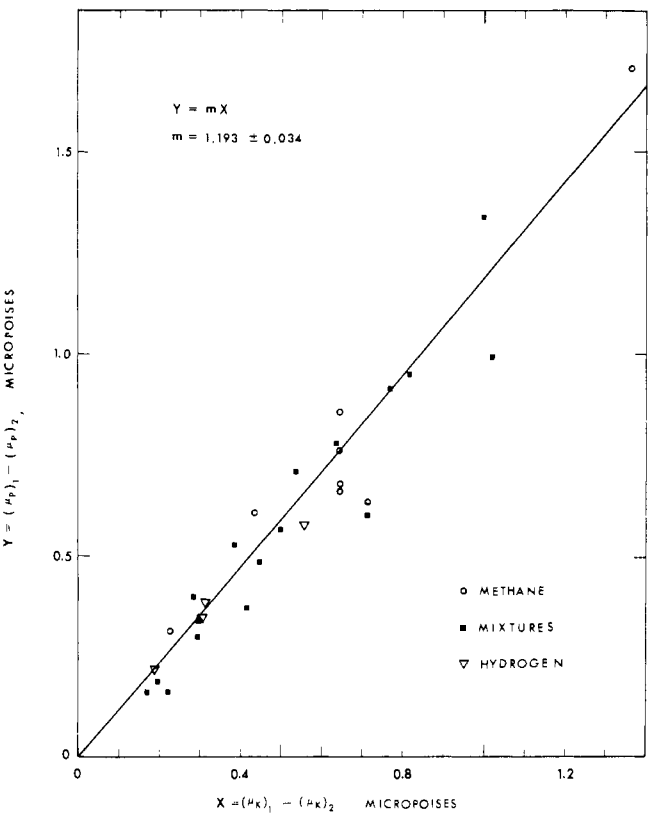

Figure 2. Graphical representation of the evaluation of the Hagenbach factor by the least-squares method.

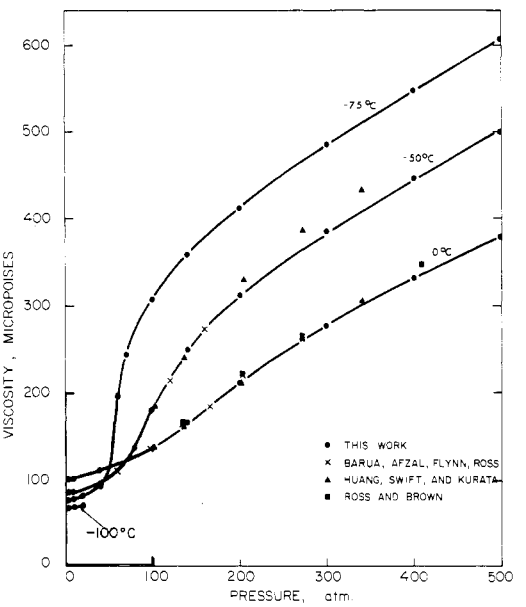

Figure 3. Isothermal behavior of the viscosity of methane from 0 to 500 atm.

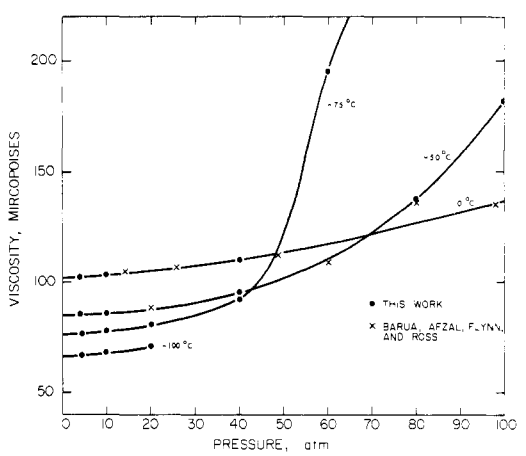

Figure 4. Isothermal behavior of the viscosity of methane up to 100 atm.

density limits of the viscosity were obtained from large scale plots of viscosity against density. The viscosity of hydrogen at 0 and −50 °C decreases slightly (0.05%) at low densities. The extrapolated intercepts, μ_0^*, are given in Table VII. The residual viscosity, $\mu - \mu_0^*$, was plotted isothermally against density for the six systems investigated. The residual viscosities for methane and mixtures A, B, and C showed no systematic temperature dependence for the whole ranges of density data. The residual concept may be regarded valid approximately (within ±1%). For hydrogen-rich mixture D and hydrogen at all densities the residual viscosity is about the same at 0 and −50 °C, but at −75 and −100 °C it is seen in Figures 10 and 11 to increase at all densities by about 0.5 to 1.0% for hydrogen and by about 1.0 to 2.0% for mixture D. This observation is higher than the accuracy of the data, which are 0.14% for the density and 0.5% for the viscosity; therefore, this temperature dependence at low temperatures for hydrogen and hydrogen-rich mixture D is apparently correct. Similar observations were made by Kao and Kobayashi (*24*) on helium at low temperature. The phenomenon may be attributed to the quantum effect of the gases.

Some calculations were made by Ghosh (*13*) in this laboratory on the viscosity data of this work which showed that a temper-

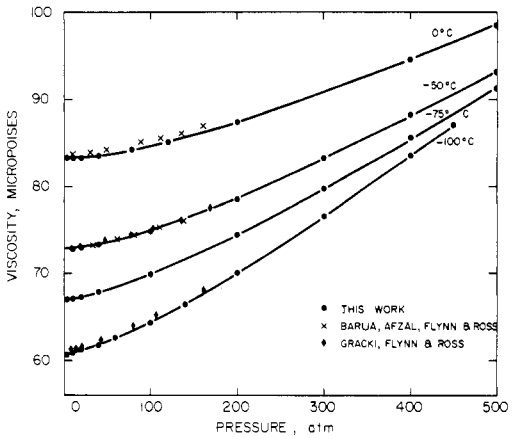

Figure 5. Isothermal behavior of the viscosity of hydrogen from 0 to 500 atm.

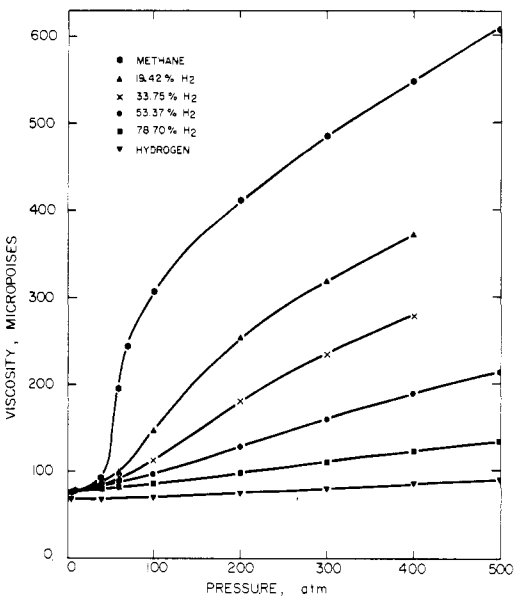

Figure 6. Example (−75 °C) of the effect of composition on the isothermal behavior for the methane–hydrogen system.

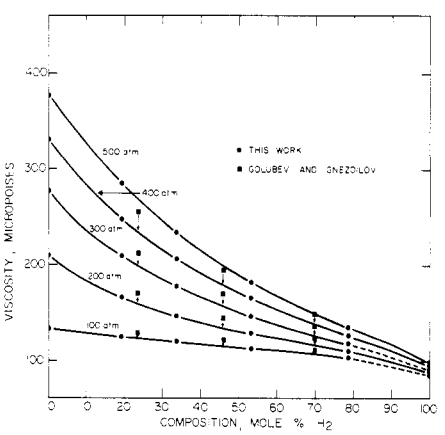

Figure 7. Isobaric behavior of the viscosity of mixtures of methane and hydrogen at 0 °C, from 100 to 500 atm.

ature dependence of the residual viscosity in the same direction for hydrogen and mixture D could be derived by using the corresponding state principle and the empirical quantum shape factors proposed by Leach et al. (*29*). However, the calculated residual viscosity vs. density curves drift from the experimental

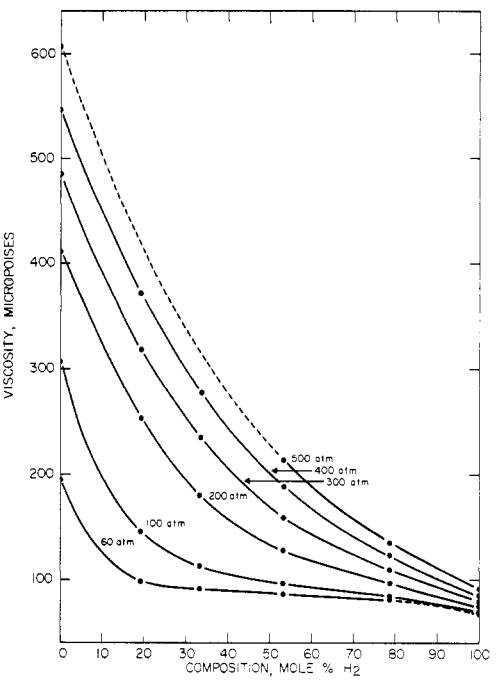

Figure 8. Isobaric behavior of the viscosity of mixtures of methane and hydrogen at −75 °C, from 60 to 500 atm.

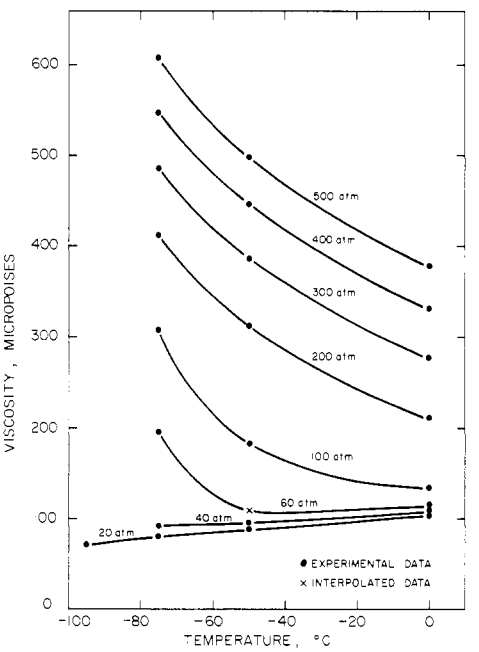

Figure 9. Isobaric behavior of the viscosity of methane from −100 to 0 °C and 20 to 500 atm.

curves systematically. Possible causes could be that the shape factors were evaluated from equilibrium properties or that the shape factor formulation is not suitable for calculating transport properties.

Comparison with Existing Data

There are no other viscosity data for CH_4–H_2 mixtures at the conditions of this work; however, several sources of data for the pure components at low temperature and high pressure are available in literature. Mixture data above 0 °C at high pressure included that of Golubev and Gnezdilov (*12*) from 0 to 100 °C up to 500 atm and that of Takahashi and Iwasaki (*19*) from 25 to 100 °C up to 500 atm.

Barua, Afzal, Flynn, and Ross (*2*) investigated both methane

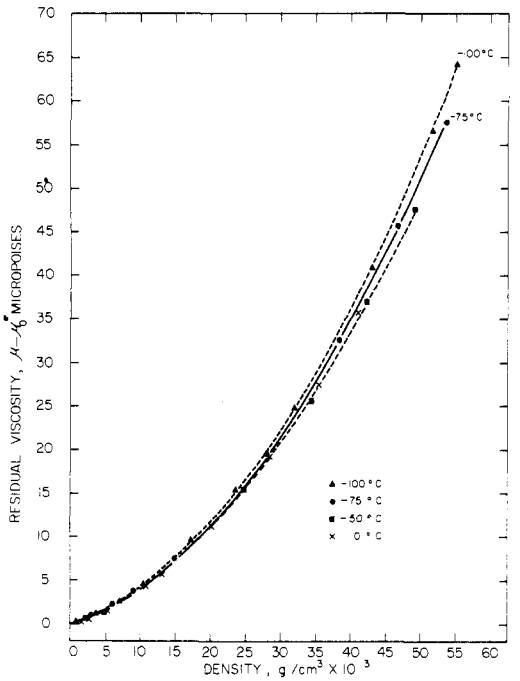

Figure 10. Residual viscosity for a 21.30% methane with 78.70% hydrogen mixture at 0, −50, −75, and −100 °C as a function of mixture density.

Table VII. Viscosity [a] of CH_4–H_2 Mixtures at Low Density Limit in Micropoises

Composition mole % H_2	Temperature, °C 0.000	−50.000	−75.000	−100.000
0	101.58	84.65	75.90	66.30
19.42	103.77	86.68	77.53	67.80
33.75	103.92	87.20	78.58	69.06
53.37	103.67	87.52	78.83	70.02
78.70	98.98	85.29	77.20	69.18
100	83.28	72.88	67.00	60.65

[a] Accuracy of viscosity ≈0.5%. One additional figure is given to avoid round off error.

Table VIII. Consideration of Critical Effect 100% Methane at −75 °C.

Pressure, atm	Flow rate $cm^3\ h^{-1}$	ΔP, mmHg	ΔP_P, mmHg	$\Delta P_P/\Delta P$
4	160	70.99	70.89	0.9986
20	120	56.605	55.91	0.9878
40	60	32.598	32.20	0.9878
40	80	43.746	42.97	0.9823
60	40	46.128	45.95	0.9961
60	50	57.844	57.38	0.9920
140	40	84.569	84.77	1.0024

and hydrogen below 200 atm from −50 to 150 °C. Gracki, Flynn, and Ross (*14*) made measurements on hydrogen from −100 to 25 °C, again below 200 atm. Capillary viscometry was also used in these works, and the precision of the data is estimated at 0.1 to 0.2%.

Two other works with lower accuracy are those of Huang, Swift, and Kurata (*17*) on methane from −170 to 0 °C up to 340 atm and of Ross and Brown (*38*) on methane from −50 to 50 °C from 34 to 500 atm.

Of these six sources listed above for comparison, two are for mixtures at higher temperatures than this work, and the other four are for the pure components, three on methane, and two

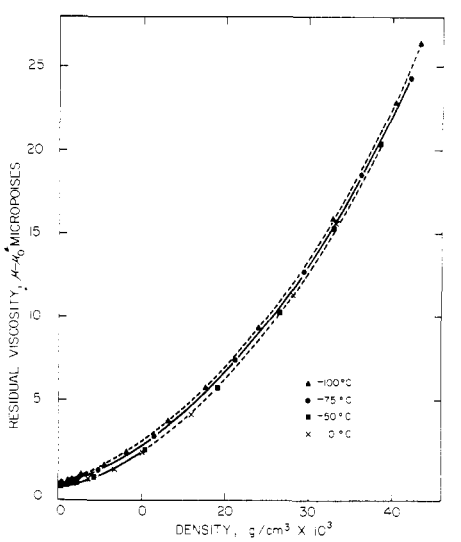

Figure 11. Residual viscosity for hydrogen as a function of density at 0, −50, −75, and −100 °C.

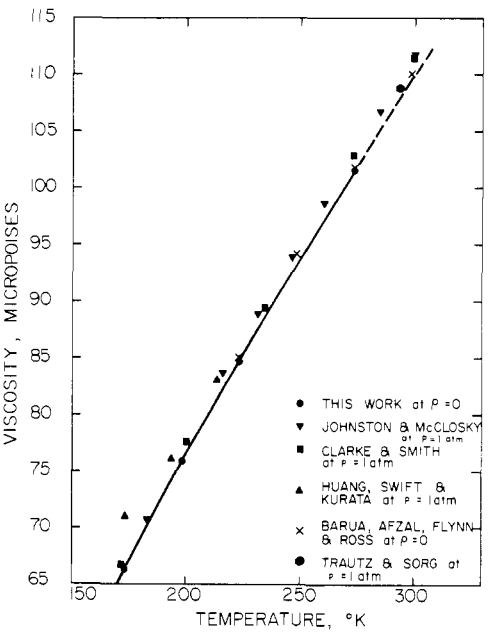

Figure 12. Viscosity at low density limit vs. temperature for methane with comparison from various sources.

on hydrogen. Comparisons were made in both viscosity–pressure and viscosity–density plots; the former is preferred since pressure is a primary measurement of the experiment.

Hydrogen. From Figure 5, it is evident that the data of Barua et al. agree well within 0.2% at −50 °C but are about 0.6% higher than this work at 0 °C. The data of Gracki et al. are from 0.3% higher at −50 °C to 0.8% higher than this work at −100 °C.

Methane. An average agreement within 0.5% is seen in Figures 3 and 4 from the data of Barua et al. at 0 °C and at −50 °C. In the work of Gracki et al., they report that the data of Barua et al. should be decreased by 0.12% based on a better calibration of the capillary diameter by the electric resistance method. In addition, they report that the experimental temperature of −50 °C reported by Barua et al. was actually −49.90 °C.

The results of Huang et al. agree well below 200 atm at 0 and −50 °C. Above 200 atm, they are about 1% higher at 0 °C and 5% higher at −50 °C. Huang et al. report an average accuracy of ±1.2%; however, examination of the original detailed data

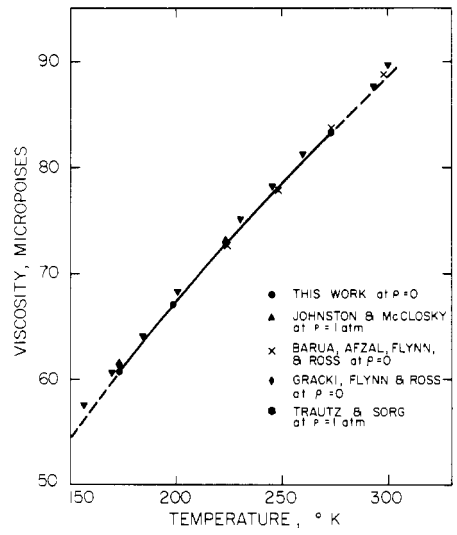

Figure 13. Viscosity at low density limit vs. temperature for hydrogen with comparison from various sources.

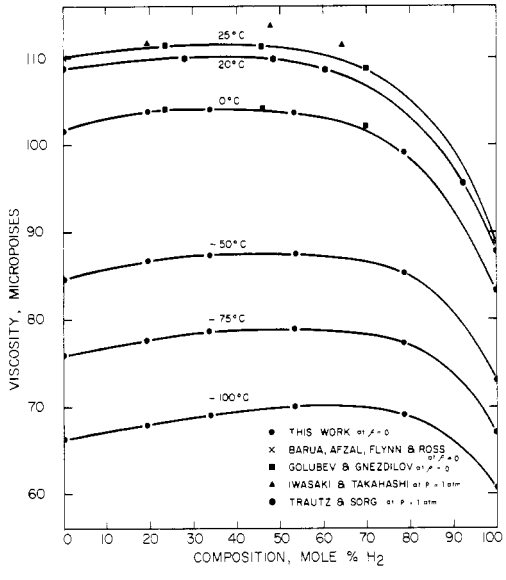

Figure 14. Viscosity of CH_4–H_2 mixtures at low density limit with comparison from other sources.

(*18*) of methane at −50 °C above 200 atm shows that the reproducibility varies from 4 to 5%. Therefore, the results of this work agree with Huang et al. within the experimental error of their work.

The data of Ross and Brown (*38*), who claim an accuracy of ±1%, are 2.3 to 4.2% higher than this work at 0 °C above 200 atm. Their data on helium and nitrogen also disagreed by more than 1% with that of Kao and Kobayashi (*24*) and Flynn et al. (*9*).

Mixtures. Only the report of Golubev et al. at 0 °C is available for comparison with this work. Their compositions were 23.6, 45.9, and 69.8% hydrogen. Their data as viscosity–pressure curves were interpolated to the pressure of this work. Their results are 2% higher at 20 atm to 7% higher at 400 atm. Their average precision was reported as ±1%.

In addition to the above comparison, the viscosity values at the low density limit are shown in viscosity–temperature plots in Figures 12 and 13 for methane and hydrogen, and in viscosity–composition plots in Figure 14 for mixtures. More viscosity values from the works of Clarke and Smith (*6*) for methane, and Trautz and Sorg (*44*) and Johnston and McCloskey (*16*) for methane and hydrogen are included for comparison.

Acknowledgments

The authors thank Dr. Don Henry for helpful discussions in the interpretation and evaluation of the data. Mr. Raymond Martin provided major assistance in the construction and adjustment of the apparatus. Phillips Petroleum Company provided the bath fluid.

Glossary

$\bar{a}$	mean radius of capillary, (7.290 77 ± 0.0002) × 10^{-3} cm
C_{PY}, C_{ST}	coefficient of temperature and pressure expansion for Pyrex and steel
L	length of capillary, 30.520 ± 0.0005 cm at 25 °C
m	Hagenbach factor
$\dot{m}$	mass flow rate
m_0	$m - 8n/\mathrm{Re}$ for $0.5 \leq \mathrm{Re} \leq 100$
$n\bar{a}$	Couette correction
P	pressure
Q_P	volumetric flow rate
q	leak correction
Re	Reynolds number
t	time
1, 2	ends of capillary
V_T	total volume of fluid system
ξ	1.000 352, nonuniformity of capillary bore
ρ	gas density at system conditions
ζ	Knudsen slip correction term
μ_P	static term in viscosity
μ_K	kinetic term in viscosity

Literature Cited

(1) Barr, G., "Monograph on Viscometry", Oxford University Press, London, 1931.
(2) Barua, A. K., Afzal, M. A., Flynn, G. P., Ross, J., *J. Chem. Phys.*, **41,** 374 (1964).
(3) Bridgman, P. W., "The Physics of High Pressure", G. Bell and Sons Ltd., London, 1952.
(4) Buffington, R. M., Latimer, W. M., *J. Am. Chem. Soc.*, **48,** 2305 (1926).
(5) Chuang, Sheng-yi, "Viscosity of Methane-Hydrogen System from −100 °C to 0 °C at Pressures up to 500 Atmospheres", Ph.D. Thesis, Rice University, Houston, Texas, April, 1972. Available from University Microfilms.
(6) Clarke, A. G., Smith, E. B., *J. Chem. Phys.*, **51,** 4156 (1969).
(7) Couette, M. M., *Ann. Chim. Phys.*, **21,** 433 (1890).
(8) Erk, S., *Z. Tech. Phys.*, **10,** 452 (1929).
(9) Flynn, G. P., Hanks, R. V., Lemaire, N. A., Ross, J., *J. Chem. Phys.*, 38, 154 (1963).
(10) Giddings, J. G., "The Viscosity of Light Hydrocarbon Mixtures at High Pressures: The Methane-Propane System", Ph.D. Thesis, Rice University, Houston, Texas, 1963. Available from University Microfilms.
(11) Giddings, J. G., Kao, J. T., Kobayashi, R., *J. Chem. Phys.*, **45,** 578 (1966).
(12) Golubev, I. F., Gnezdilov, N. E., *Teplooenergetika,* **14,** 93 (1967).
(13) Ghosh, A. K., private communication, Rice University, Houston, Texas, 1972.
(14) Gracki, J. A., Flynn, G. P., Ross, J., *J. Chem. Phys.*, **51,** 3856 (1969).
(15) Hagenbach, E., *Pogg. Ann.* **109,** 385 (1860).
(16) Henry, D. L., private communication, Rice University, Houston, Texas, 1974. See also Kim, D. M. Henry, D. L., Kobayashi, R., *Phys. Rev. A.* **10,** 1808 (1974).
(17) Huang, E. T. S., Swift, G. W., Kurata, F. *AIChE J.*, **12,** 932 (1966).
(18) Huang, E. T. S., Swift, G. W., Kurata, F., Preprint 29B, AIChE 58th National Meeting, 1966.
(19) Iwasaki, H., Takahashi, H., *Bull. Chem. Res. Inst. Non-aqueous Solutions, Tohoku Univ.*, **10,** 81 (1961).
(20) Johnston, H. L., Altman, H. W., Rubin, T., *J. Chem. Eng. Data,* **10,** 241 (1965).
(21) Johnston, H. L., McCloskey, K. E., *J. Phys. Chem.*, **44,** 1038 (1940).
(22) Kalekar, A. S., Kestin, J., *J. Chem. Phys.*, **52,** 4248 (1970).
(23) Kao, J. T., "Viscosity of Helium-Nitrogen Mixtures at Low Temperatures and High Pressures", Ph.D. Thesis. Rice University, Houston, Texas, 1966. Available from University Microfilms.
(24) Kao, J. T., Kobayashi, R., *J. Chem. Phys.*, **47,** 2836 (1967).
(25) Kao, J. T., Ruska, W., Kobayashi, R., *Rev. Sci. Instrum.*, **39,** 824 (1968).
(26) Kestin, J., Leindenfrost, W., *Physica (Utrecht),* **25,** 1033 (1959).
(27) Kestin, J., Sokolov, M., Wakeman, W., *Appl. Sci. Res.*, **27,** 241–264 (1973).

(28) Knudsen, M., *Ann. Phys.*, **28,** 75 (1909).
(29) Leach, J. W., Chappelear, P. S., Leland, T. W., "Properties of Hydrocarbon and Quantum Gas Mixtures from the Corresponding States Principle", *Proc. Amer. Pet. Inst., Sect. 3,* **46,** 223 (1966).
(30) Michels, A., Gibson, R. O., *Proc. R. Soc. London, Ser. A,* **134,** 288 (1931).
(31) Michels, A., deGraff, W., Wassenaar, T., Levelt, J. M. H., Louwerse, P., *Physica (Utrecht),* **25,** 25 (1959).
(32) Michels, A., Schipper, A. C. J., Rintoul, W. H., *Physica (Utrecht),* **19,** 1011 (1953).
(33) Mueller, W. H., Leland, T. W., Kobayashi, R., *AIChE J.,* **7,** 267 (1961).
(34) Poiseuille, J., *Memories des Savants etangers,* **9,** 433 (1846).
(35) Pope, G. A., Chappelear, P. S., Kobayashi, R., *AIChE J.,* **22,** 191 (1976).
(36) Rankine, A. O., *Proc. R. Soc. London, Ser. A,* **84,** 181 (1911).
(37) Rankine, A. O., *Proc. R. Soc. London, Ser. A,* **83,** 265 (1910).
(38) Ross, J. F., Brown, G. M., *Ind. Eng. Chem.,* **49,** 2026 (1957).
(39) Ruska, W. E. A., Carruth, G. F., Kobayashi, R., *Rev. Sci. Instrum.* **43,** 1331 (1972).
(40) Ruska, W., Kao, J., Chuang, S. Y., Kobayashi, R., *Rev. Sci. Instrum.,* **39,** 1889 (1968).
(41) Sutherland, B. P., Maass, O., *Can. J. Res.,* **6,** 428 (1932).
(42) Thornton, S. J., Dunlop, P. J., *Chem. Phys. Lett.,* **23,** 203 (1973).
(43) Trautz, M., Baumann, P. B., *Ann. Phys.,* **2,** 733 (1929).
(44) Trautz, M., Sorg, K. G., *Ann. Phys.,* **10,** 81 (1931).
(45) Trautz, M., Weizel, W., *Ann. Phys.,* **4,** 305 (1925).
(46) Vennix, A. J., Leland, T. W., Kobayashi, R., *AIChE J,* **15,** 926 (1969).
(47) Weissberg, H. L., *Phys. Fluids,* **5,** 1033 (1962).

Received for review August 18, 1975. Accepted July 10, 1976. Financial support was provided by the National Science Foundation, the Monsanto Company, and Rice University.

Extinction Coefficients of Chlorine Monoxide and Chlorine Heptoxide

Chorng-Lieh Lin
Jet Propulsion Laboratory, California Institute of Technology, Pasadena, California 91103

The ultraviolet and visible extinction coefficients of Cl_2O and Cl_2O_7 were measured from 180 to 800 nm. The results are comparable in shape with literature values, but different in magnitude. The approximate extinction coefficients at the peaks of infrared absorption lines are also given.

Recent laboratory measurements and model atmospheric calculations (*8, 10, 13, 15*) point to possible adverse effects of chlorine-containing compounds in the stratosphere, particularly the destruction of ozone. As part of our study of chlorine–ozone chemistry (*8*), we have synthesized various chlorine oxides and have measured their extinction coefficients. Some of these oxides may be products or intermediates in the chlorine–ozone reaction system. We report here the extinction coefficients of Cl_2O and Cl_2O_7 in the ultraviolet, visible, and infrared spectral regions.

The extinction coefficients ϵ were defined as

$$\log I_0/I = \epsilon c l$$

where the concentration c is in moles/liter, the optical path length l is in cm, and $\log I_0/I$ is the absorbance.

The absorption spectra in the ultraviolet and visible regions were taken with a Cary 15 spectrophotometer (Applied Physics) using a quartz absorption cell of 10-cm path length. Wavelength calibrations were accomplished by using O_2 Shumann-Runge absorption bands (*1, 3*) near 180 nm, and mercury low pressure lines at longer wavelengths.

The ir absorption spectrum was recorded with a Perkin-Elmer Model 21 double beam spectrophotometer from 650 to 5000 cm^{-1} with resolution set at 927. At this setting, the spectral band-passes at different wavelengths are known and supplied by the manufacturer. The absorption cell was made of Pyrex glass with NaCl windows.

A fused quartz precision pressure gauge (Texas Instruments) was used for pressure measurements. The accuracy of the pressure measurements was better than 1%.

(A) Cl_2O

The chlorine monoxide was prepared (*11*) by slowly passing Cl_2 (Matheson research grade) through a reaction tube packed with mercuric oxide (Allied Chemical) which had been previously heated under vacuum to about 250 °C. Chlorine monoxide was condensed in a U-tube surrounded by a solid–liquid slurry of ethanol at ca. −117 °C. Trap-to-trap purification was performed at −117 °C to ensure purity. Since Cl_2O absorption extends into the visible region, special caution was taken to guard against possible photodecomposition resulting from exposure of the purified sample to room light. The purity of chlorine monoxide used in the extinction coefficient measurements was estimated from its stoichiometric ratio determination using pressure measurements before and after complete decomposition into Cl_2 and O_2. This ratio is 2:0.986 compared to the theoretical value of 2:1, indicating that Cl_2O purity is better than 98.5%. Cl_2O was readily decomposed into Cl_2 and O_2 by low pressure mercury lamp irradiation. The amount of Cl_2 produced after decomposition could also be calculated from its peak absorption near 330 nm, with known extinction coefficient (*12*), and the amount of O_2 could be roughly measured from the Shumann-Runge absorption bands. These absorption measurements confirmed the correctness of the aforementioned purity estimate. The absence of absorption characteristic of other chlorine oxides attested further to the purity of the Cl_2O.

Six samples of Cl_2O with pressures ranging from 1 to 165 Torr were used for extinction coefficient measurements. No absorption was recorded for wavelengths greater than 650 nm when the samples were scanned from 800 to 180 nm. Little effect was observed when Cl_2O samples were pressurized to 760 Torr with N_2 gas. These results in the uv and visible are summarized in Table I and plotted in Figure 1 along with the values of Goodeve and Wallace (*6*) and of Finkelnburg, Schumacher, and Stieger (*4*) for comparison. Although all three data sets are of the same shape, the differences in value at various wavelengths are apparent. The accuracy of the uv extinction coefficients measured in the present work is estimated to be about 5% in the region of main interest, between 180 and 330 nm. In the region between 330 and 470 nm it is 10% and at wavelengths greater than 470 nm, the uncertainty is probably greater than 10% because of weak absorption.

The ir approximate extinction coefficients at the peaks (*9*) of absorption lines along with their spectral band-passes are given in Table II. Again, little effect on extinction coefficient was observed when the Cl_2O sample was pressurized to 760 Torr with N_2 gas.